EXPERIMENTAL INVESTIGATION OF STEEL BRACES INSTALLED WITH INTENTIONAL ECCENTRICITY USING GUSSET PLATE CONNECTIONS

K. Skalomenos[1], H. Inamasu[2], H. Shimada[3], M. Kurata[4] and M. Nakashima[5]

[1] *JSPS Postdoctoral fellow, DPRI, Kyoto University, Gokasho, Uji, Kyoto 611-0011, Japan, skalomenos.konstantinos.28r@st.kyoto-u.ac.jp*

[2] *JSPS Doctoral student, DPRI, Kyoto University, Gokasho, Uji, Kyoto 611-0011, Japan, hiro.inamasu@gmail.com*

[3] *Master student, DPRI, Kyoto University, Gokasho, Uji, Kyoto 611-0011, Japan, shimada.hironari.25e@st.kyoto-u.ac.jp*

[4] *Associate Professor, DPRI, Kyoto University, Gokasho, Uji, Kyoto 611-0011, Japan, kurata.masahiro.5c@kyoto-u.ac.jp*

[5] *Professor, DPRI, Kyoto University, Gokasho, Uji, Kyoto 611-0011, Japan, nakashima@archi.kyoto-u.ac.jp*

Abstract

The present paper proposes an improved design of conventional buckling braces (CBBs) by introducing intentional eccentricity along the brace length. The proposed brace is named the Brace with Intentional Eccentricity (BIE). Due to the inherent action moment caused by the eccentrically applied axial force, the BIE bends uniformly form small story drifts and sustains tri-liner behavior under tension, while under compression moves smoothly into the post-buckling behavior. BIE provides independent design of strength and stiffness, large post-yielding stiffness and high ductility by delaying the appearance of mid-length local buckling. The present experimental study consists of three specimens subjected to cyclic flexural load protocol with variable intensities from 0.10% to 4.0% story drift angle. Gusset plate connections designed to accommodate inelastic rotations were used to connect the bracing members in the loading frame. Different values of the applied eccentricity were tested and comparisons with a CBB were made to examine and evaluate various aspects of the BIE cyclic behavior.

Keywords: Eccentricity; Steel brace; Gusset plate; Ductility; Cyclic behavior

1. Introduction

Steel braces provide additional strength and stiffness for building structures to control the lateral drift and dissipate energy in their mid-length by means of inelastic deformations. The most common steel bracing systems are the conventional buckling braces (CBBs). However, CBBs are characterized by intense local buckling in the middle of their length, which leads to unstable energy dissipation and finally to fracture [1, 2] and offer very limited post-yielding stiffness. Large post-yielding stiffness is beneficial to reduce strength and residual displacement demand in structures [3] and to prevent the soft-story mechanism [4]. Finally, in the design of CBBs, strength and stiffness are functions of the cross-section and cannot be assigned independently. As a result, strength demands often lead to very large stiffness, which in turn increases the base shear and seismic acceleration.

To overcome the weaknesses obtained from conventional steel braces, the present paper proposes a new and prototype design of CBBs aimed to improve their seismic performance by forming the initial stiffness separately of the maximum strength capacity, by increasing the post-yielding stiffness and by delaying the occurrence of local buckling. These phenomena are naturally and simply controlled by introducing along the brace length eccentricity e, as shown in Fig. 1(a). Steel braces with intentional eccentricity, called the BIE, deform from a small story drift due to the moment caused by the eccentrically applied axial force. Fig. 1(b) depicts the deformation mechanism of the BIE in both tensile and compressive forces. Under tension two plastic hinges are created at the brace ends and the eccentricity in the middle becomes zero. At that time, the steel brace is subjected to pure tension. Under compression, the brace buckles uniformly having an arc-shaped deformation and a plastic hinge is created in the mid-length. Because of this deformation mechanism, the BIE appears different response characteristics compared with the CBB. Fig. 1(c) compares the backbone curves of the two different braces, assuming that CBB exhibits an ideally bilinear behavior under tension. In comparison with CBB, the BIE displays tri-linear behavior under tension and under compression the elastic part is not followed by an abrupt post-buckling non-linear curve. By applying eccentricity, the initial stiffness and yield strength are reduced and the post-yielding stiffness appreciably increases. The ultimate tensile strength remains the same with the corresponding conventional brace of the same cross section. In addition, due to the overall bending behavior caused by the inherent moment, stresses and strains are distributed more uniformly along the brace length. The strain concentration at the middle delays and the member's life is significantly extended.
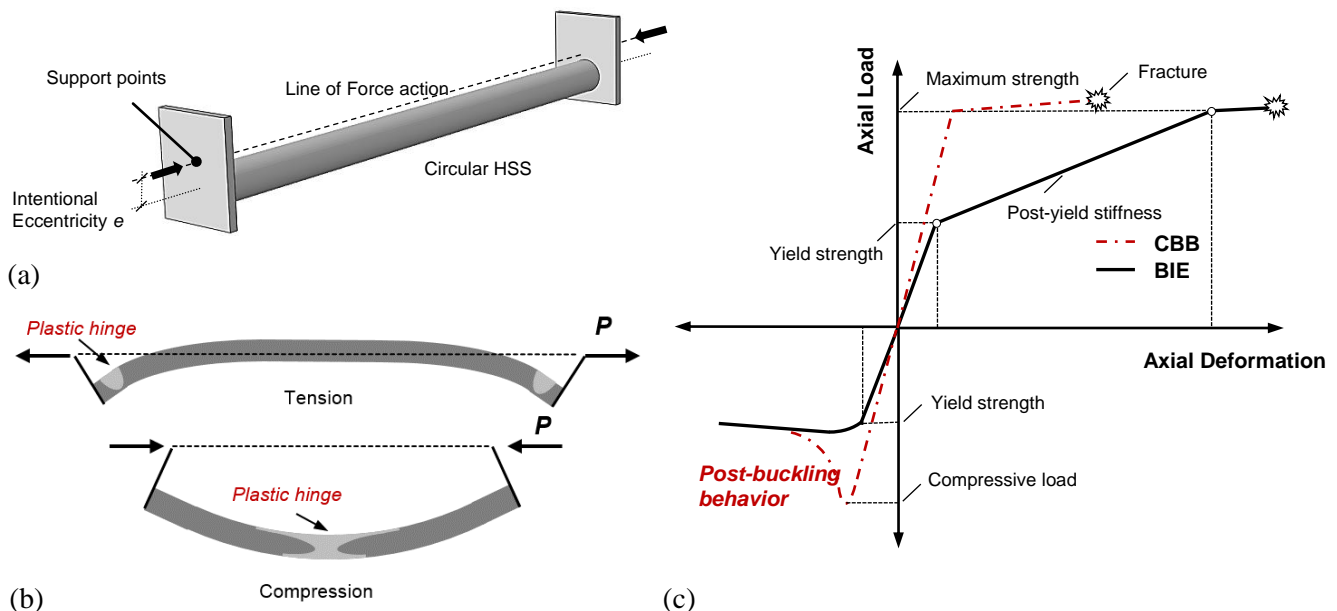
Fig. 1 – Overview of proposed steel brace: (a) BIE configuration; (b) defromed shape under tesnion and compression; and (c) backbone curves of CBB and BIE

2

This paper presents experimental work on the proposed steel brace. Three half-scaled specimens were subjected to a cyclic lateral loading protocol with variable intensities for drift angles ranging from 0.10% to 4.0%. Gusset plates designed following the recommendations of Ref. [5] to accommodate inelastic rotations were used to connect the bracing members in the surrounding loading frame. Several values of the applied eccentricity were examined and comparisons with a conventional specimen were made to evaluate various aspects of the BIE cyclic behavior. Based on the test results, the initial stiffness of BIE was reduced up to 56%, the post-yielding stiffness was ranged from 14% to 18% of the initial stiffness, and the local buckling and the fracture were delayed up to high drift levels (2.0% and 3.0% story drift, respectively).

2. Test Plan

Table 1 shows design details of the specimens, including material properties of the steel tubes and gusset plates, while Fig. 2(a) shows the test specimen dimensions. A compact circular hollow steel section with diameter (D)-to-thickness (t_b) ratio equal to 32.7 was adopted for the braces made of conventional Japanese STK400 steel (equivalent to A36 in the United States for hollow sections). All steel tubes had a length of 1575 mm and a slenderness ratio $\lambda = 54.4$. The gusset plates were fabricated from a steel plate made of conventional Japanese SS400 steel (equivalent to A36 in the United States for steel plates) having thickness (t_p) of 12 mm. The gusset plates were designed using the $2t_p$ clearance distance and they had a tapered shape with width (W) varying from 277 to 244 mm. All the welded areas of the connections were manufactured using complete-joint-penetration welds. The test specimens and connections were designed following the recommendations of Ref. [5].

Table 1 – Dimensions and material properties of test specimens

Specimen	Steel tubes						Gusset plate		
	D (mm)	t_b (mm)	E (mm)	e/r	F_y / F_u (MPa)	λ	W (mm)	t_p (mm)	F_y / F_u (MPa)
S1-e60	114.3	3.5	60	1.53	328.6/490	54.40	277	12	308.2/446.5
S1-e30	114.3	3.5	30	0.77	328.6/490	54.40	277	12	308.2/446.5
S1-e0	114.3	3.5	0	0.0	328.6/490	54.40	277	12	308.2/446.5
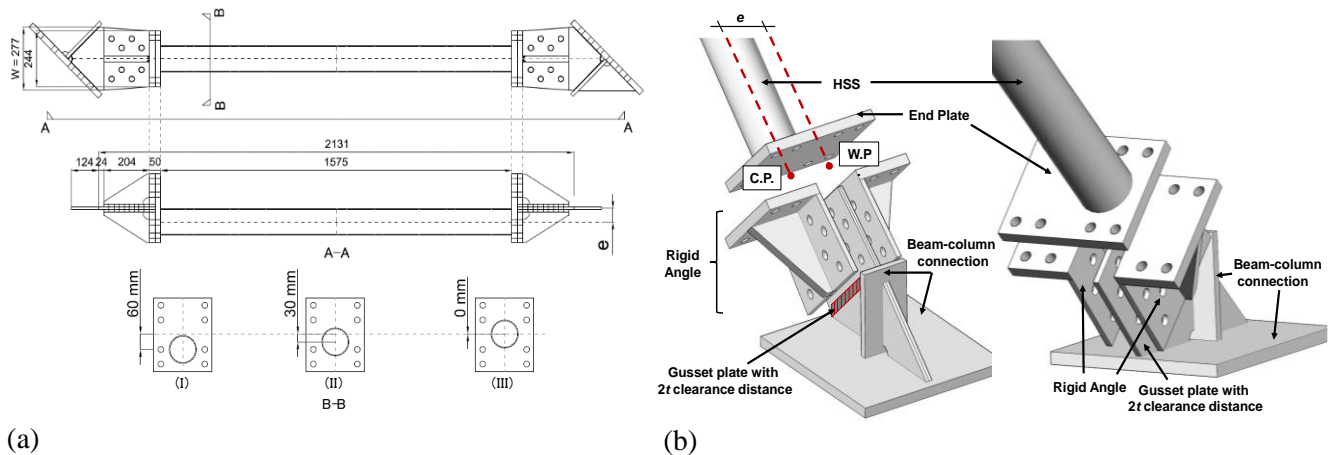
Fig. 2 – Test specimen: (a) brace dimension; (b) details of GP connection

To study the effect of eccentricity, eccentricities equal to 30 mm and 60 mm were adopted; the e/r ratios were 0.77 and 1.53, respectively, where r is the radius of gyration of the cross-section (Table 1). The test results were compared with those of the conventional specimen for which no eccentricity was adopted. Based on nonlinear finite element analysis [6], the 60 mm eccentricity ensures that the maximum tensile strength (Fig. 1(a)) is reached at a story drift of about 3%, where relatively large ductility is achieved. The 30 mm eccentricity was chosen so that the brace reaches its ultimate strength at nearly 1.0% story drift.

Fig. 2(b) shows the proposed configurations of the gusset plate connection. The connection mainly consists of three parts: a) a gusset plate with a clearance distance twice its thickness, b) two rigid angles placed on either side of the gusset plate, and c) one end plate welded at the brace end. The two rigid angles consist of two steel plates arranged in an L-shape, and their rigidity is ensured by a steel stiffener. One surface of these rigid angles is connected to the brace through the end plate, while the other is connected directly to the gusset plate. Because of these two rigid angles, the inelastic deformations are concentrated directly within the clearance distance of the gusset plate forming a plastic hinge. This plastic hinge helps the BIE to buckle out-of-plane and to achieve the desired behavior as described in Fig. 1. The flat surface of the end plate allows any value of eccentricity e to be adopted. All aforementioned connection parts are connected together by high-strength bolts.

Fig. 3 shows the test setup and the surrounding loading frame. The specimen was arranged in the four-pin frame at a 45° angle. A cyclic load was applied by imposing varying lateral displacements at the top of the frame with the aid of an oil jack fixed to a steel reaction wall. The lateral loading history comprised several drift angle levels (0.1%, 0.25%, 0.5%, 1%, 2%, 3%, 4%, each imposed for two cycles). The axial displacement was calculated as the average of displacements measured by linear displacement transducers located on either side of the brace. A good number of linear displacement transducers were also placed along the brace length to record the deformed shape of the braces. In addition, longitudinal strain gauges were mounted on the specimens at critical points. The lateral load was measured using a load cell at the loading point.
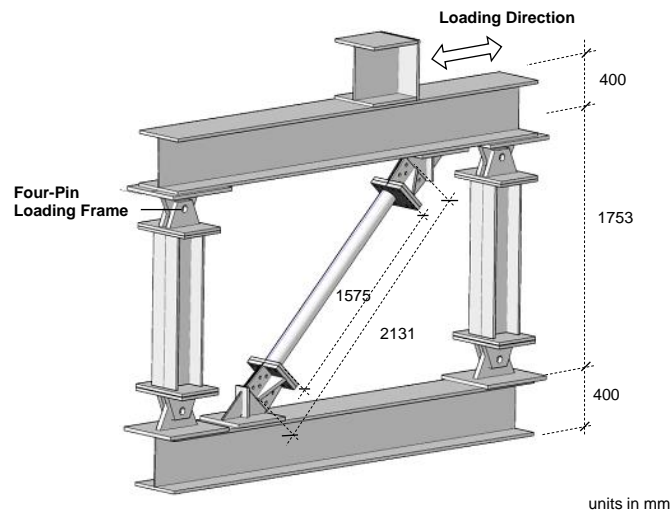
Fig. 3 – Test setup and loading frame

3. Test Results and Observations

Hysteresis curves of the lateral load versus lateral story drift are shown in Fig. 4 for the three specimens examined here. Table 2 also gives experimental values of important quantities, such as the elastic stiffness, tensile and compressive yield strengths, post-yielding stiffness, and ultimate strength. In Table 2, the tensile and compressive yield strengths were based on the strain gauge measurements at first yielding. The post-yielding stiffness was calculated using the force–displacement values that correspond to the points of tensile yielding and maximum tensile strength. Drift levels at which local buckling and fracture occurred are also provided in Table 3.
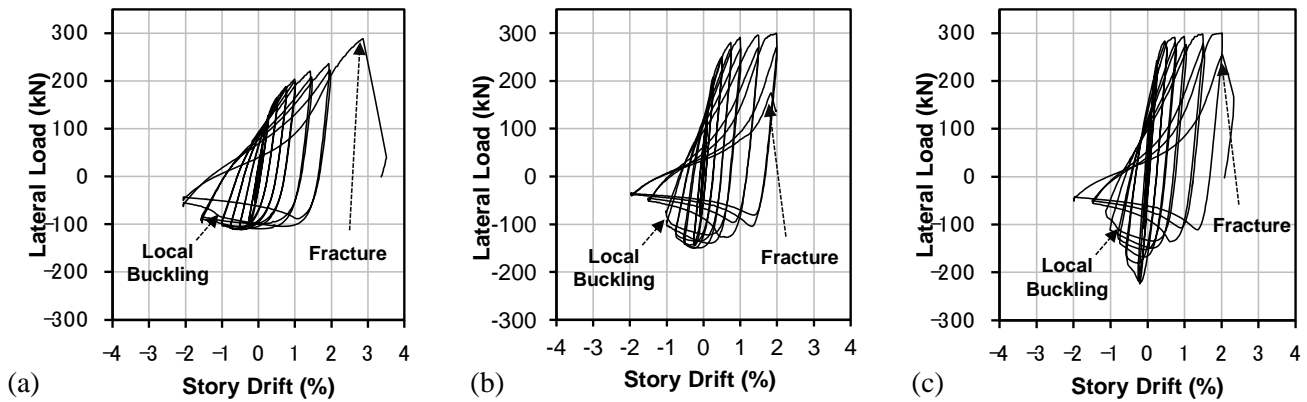
Fig. 4 – Hysteresis curves of the three test specimens: (a) S1-e60; (b) S1-e30; and (c) S1-e0

3.1 Cyclic behavior of BIE

In this section the cyclic behavior of BIE is discussed by explaining the cyclic behavior of the specimen S1-e60 with 60mm eccentricity [Fig. 4(a)]. The specimen began to dissipate energy at a force half than that of conventional S1-e0 (CBB) specimen (Table 2), and up to 2% story drift, its behavior was stable without pinching phenomena or significant strength deterioration. Because of early yielding, large post-yielding stiffness of almost 14% of the initial stiffness was provided under tension. The BIE reached its maximum tensile strength at nearly 3.0% story drift, where the eccentricity in the middle section was reduced almost to zero (Fig. 1b). Under compression, the specimen transitioned smoothly into post-buckling behavior, avoiding a severe drop in compressive strength, and an almost elastoplastic behavior was observed up to 1.5% story drift. In the first compression cycle of 2.0% drift, local buckling was observed which led to pinching and deteriorating behavior.

Table 2 – Test results of important design quantities

Specimens	Elastic Stiffness (kN/mm)	Tensile Yield Strength (kN)	Yield Drift (%)	Post-yield Stiffness (kN/mm)	Max. Strength (kN)	Max. Strength Drift (%)	Comp. Strength (kN)
				Important quantities			
S1-e60	28.62	97.5	1st 0.2[0.19]	3.84	286.2	3.0	-90.5
S1-e30	53.62	147.0	1st 0.25[0.14]	9.34	287.8	1.0	-130.6
S1-e0	65.54	222.6	1st 0.25[0.24]	0.60	284.2	0.4	-209.1

1st 0.25 [0.19]: 1st denotes the loading cycle; 0.25 denotes the story drift level; [0.19] denotes the exact measured drift angle

Table 3 – Drift levels at which local buckling and fracture occurred

Specimens	Drift levels (%) of failure modes	
	Local Buckling	**Fracture**
S1-e60	1st -2.0 [-1.09]	1st 3.0 [2.87]
S1-e30	2nd -1.0 [-1.0]	1st 3.0 [1.80]
S1-e0	2nd -1.0 [-0.75]	2nd 2.0 [2.0]

1st -2.0 [-1.09]: 1st denotes the loading cycle; -2.0 denotes the story drift level; [-1.09] denotes the exact measured drift angle

Compared with the CBB, a notable delay of the occurrence of local buckling was observed for the BIE. Fig. 5 shows the deformation of the S1-e0 (CBB) and S1-e60 (BIE) specimens in the middle cross section under the second compression cycle of 1.0% story drift. Local buckling in the mid-length of the CBB combined with intense overall out-of-plane buckling were occurred at this drift level, while no damage was observed in the BIE at the same drift level which had a slighter and more uniform overall deformation. Owing to the moment contribution, the overall deformation was more uniform in the BIE specimen, thus delaying the strain concentration in the middle. Local buckling occurred in the BIE at 2.0% story drift, which is a drift level two times larger than that at which local buckling occurred in the CBB.

(a)   (b)
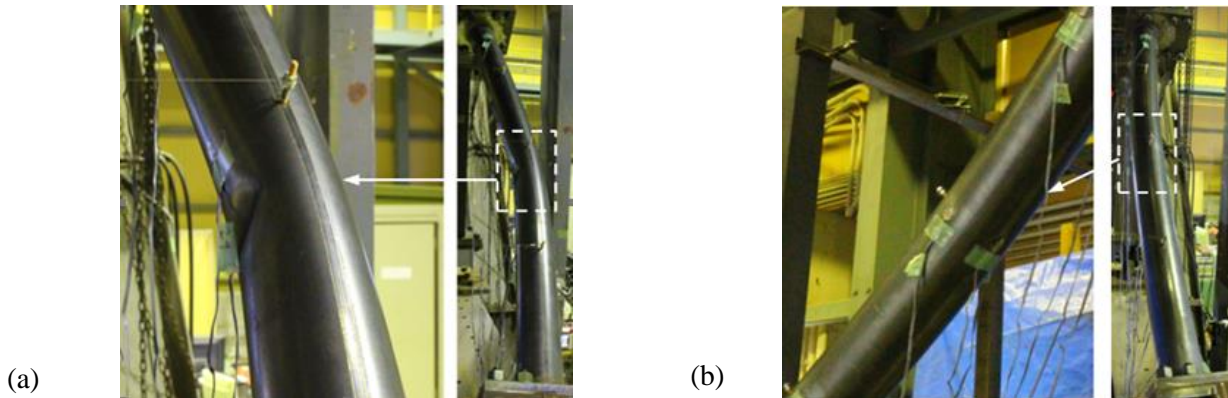
Fig. 5 – Second compression cycle of 1.0% story drift: (a) S1-e0 (CBB); and (b) S1-e60 (BIE)

3.2 Effect of eccentricity

As shown in Table 2, the elastic stiffness of the CBB specimen (S1-e0) was 65.54 kN/mm, that of 30mm-eccentricity (S1-e30) was 53.62 kN/mm, and that of 60mm-eccentricity (S1-e60) was 28.62 kN/mm. The yielding of the steel tube occurred during the first tensile cycle of the 0.25% drift level and was observed at the following specific story drifts: (a) 0.24% for S1-e0, which corresponds to a yield strength of 222.6 kN; (b) 0.14% for S1-e30, which corresponds to a yield strength of 147.0 kN; and (c) 0.19% for S1-e60, which corresponds to a yield strength of 97.5 kN. The post-yielding stiffnesses of the specimens were 0.60, 9.34 and 3.84 kN/mm, respectively. The specimens reached an almost identical maximum lateral force at 0.4%, 1.0% and 3.0% story drift levels, respectively.

Compared with the CBB specimen, in BIE specimens, the elastic stiffness decreased by 18.2% by applying 30mm eccentricity and by 56.3% by applying 60mm eccentricity. These results clearly indicate that desired values for the initial stiffness can be assigned without changing the maximum strength of the brace. Another benefit is the high post-yielding stiffness. The post-yielding stiffness of the specimens with 30- and 60-mm eccentricity was 17.4% and 13.4% of the initial stiffness, respectively, while that of the CBB was barely 1% of the initial stiffness.

Regarding the failure modes, local buckling was observed in the mid-length during the second compressive cycle of the 1% story drift in the conventional specimen, at the end of the same cycle in the BIE specimen with 30 mm eccentricity, and during the first compressive cycle of the 2% story drift in BIE specimen with 60 mm eccentricity. The local buckling was followed by the fracture of steel tubes. More specifically, fracture occurred during the second tensile cycle of the 2% story drift in the conventional specimen and during the first tensile cycle of the 3% story drift in the BIE specimen of 30 mm eccentricity. Fig. 6(a) shows the fracture of the 30mm-eccentricity specimen at the mid-length. The BIE specimen of 60 mm eccentricity failed by fracture at the upper brace end [Fig. 6(b)] at the end of the first tensile cycle of the 3% story drift level, when the specimen reached its maximum tensile force [Fig. 4(a)]. This drift level is 1.5 times larger than that at which fracture occurred in CBB. Fracture occurred at the brace end in this BIE specimen due to the larger rotation demand required by the eccentricity of 60 mm. As discussed in Fig. 1(b), two plastic hinges are formed at the brace ends under tension which rotate until the eccentricity in the middle becomes zero. However, the fact that

no crack was occurred at the mid-length at this drift level indicates that the member's life can be extended further by strengthening the brace ends. The failure was occurred in the heat affected zone (HAZ) next to the welding line. The test results showed that as eccentricity increases, the ductility of the BIE increases owing to the delay of the occurrence of local buckling and fracture in the mid-length. A subject of future study is the development of a connection that ensures no fracture at the brace ends when large values of e/r are adopted.

(a)

(b)
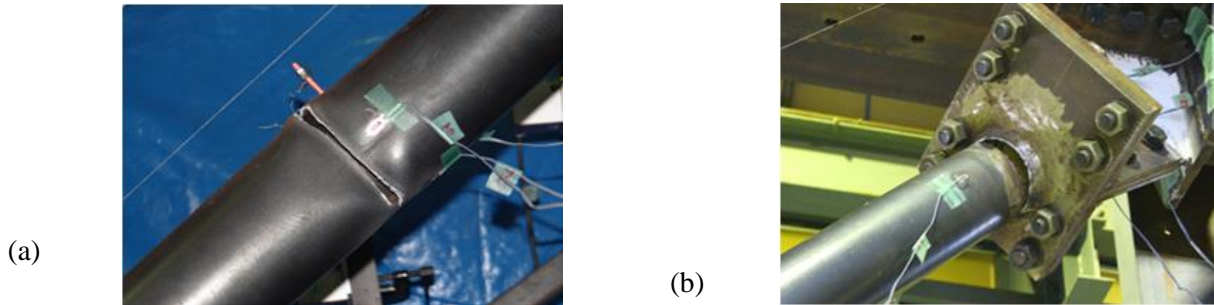
Fig. 6 – Failure modes of BIE specimens: (a) brace middle of the specimen S1-30 at 2% tension drift; and (b) brace end of the specimen S1-60 at 3% tension drift

4. Conclusion

Major findings of this experimental study are as follows:

1. In the proposed design scenario for steel braces, stiffness and strength can be designed independently. Compared with a CBB of the same cross-section, the proposed steel brace offers 18.2% and 56.3% reduced stiffness for $e/r = 0.77$ and $e/r = 1.53$, respectively, and identical maximum tensile strength.

2. Tri-linear behavior characterizes the response of the proposed brace under tension. The BIE began to dissipate energy at a smaller force than that of CBB, is able to provide larger post-yielding stiffness close to 18% of the initial stiffness, and can stably dissipate energy up to 2% story drift. Under compression, the BIE moves smoothly into the post-buckling behavior experiencing approximately a bi-linear behavior.

3. The test results show that as the eccentricity increases the ductility of the proposed brace increases owing to the delay of occurrence of local buckling and fracture in the mid-length. In the BIE specimen of $e/r = 1.53$, local buckling and fracture occurred at a story drift level 1.5 to two times larger than that at which local buckling and fracture occurred in the CBB.

5. References

[1] Tremblay R (2002): Inelastic seismic response of steel bracing members. *Journal of Constructional Steel Research*, 58(5-8), 665–701.

[2] Fell BV, Kanvinde AM, Deirlein GG, Myers AT (2009): Experimental Investigation of Inelastic Cyclic Buckling and Fracture of Steel Brace. *Journal of Structural Engineering - ASCE*, **135** (1), 19–32.

[3] García RJ, Miranda E (2003): Inelastic displacement ratio for evaluation of exisaiting structures. *Earthquake Engineering & Structural Dynamics*, **32** (8), 1237–1258.

[4] Merczel BD, Aribert J-M, Somja H, Hjiaj M, Lógó J (2015): On the weak store behavior of concentrically braced frames. *8th International Conference on Behavior of Steel Structures in Seismic Areas STESSA'15*, Shanghai, China.

[5] AISC (American Institute of Steel Construction) (2010): *Specification of structural steel buildings*. ANSI/AISC Standard 360-10, Chicago.

[6] Simulia (2014): *Abaqus/CAE User's Manual Ver. 6.14*. Hibbitt, Karlsson, & Sorensen, Inc., Providence, RI, USA.